Modeling and Control of Magnetic Flexible Rotor Bearing System

C.S. Toh[1], S.-L. Chen[1], P.-L. Wang[2], and D. Juang[2]

[1] *Advanced Institute of Manufacturing with High-tech Innovations and Department of Mechanical Engineering, National Chung Cheng University, Chia-Yi 621, Taiwan, ROC*

[2] *Materials & Electro-Optics Research Division, Chung-Shan Inst. of Science and Tech., Taiwan, ROC*

imeslc@ccu.edu.tw

Abstract - The two ways of developing a model of flexible rotor in AMBs which established in this study are generalized polynomial expansion method (G.P.E.M) and the so-called Eigen Mode Method. In Eigen Mode Method, a set of basic functions for non-uniform rotating rotor are required, and Generalized Polynomial Expansion Method is applied to compute numerical solutions. At last, we able to represent the overall system by a lower order model, and the orthogonality of basic functions are higher priority, it will cause performance of model reduction directly. In issue of controller design, feedback linearization and Integral Sliding Mode Control (ISMC) are applied to overcome the effect of nonlinearity and uncertainty. The feedback linearization is based on perfect models, which are almost impossible to exist in practice. A more reasonable assumption is that real system model is nominal one plus a bounded uncertain part. In this study, an integral sliding mode controller will be designed to allow for large uncertainties and to achieve good steady-state accuracy. Simulations are carried out to verify the proposed modeling method and robust controller for magnetic flexible rotor bearing system. The main concerns are the performances in various influences of uncertainties caused by unmodeled dynamics.

Keywords – flexible rotor, active magnetic bearing.

I. INTRODUCTION

Active magnetic bearings (AMBs) represent a preferred alternative to conventional mechanical bearing designs in a variety of machinery applications as grinding machines, vacuum pumps and energy storage flywheel system. Some conditions such as extreme temperature, corrosive working fluids, and extreme cleanliness often preclude the use of conventional lubricated bearings. With implementing an AMBs system, the advantages include: complete elimination of oil-based lubrication systems, low parasitic loss, lower maintenance costs and longer system life. Because AMBs enables to support rotor without friction, and it is widely applied to high-speed rotors.

However, as the rotation speed of rotor increases, more elastic modes of rotor which caused by gyroscopic effect appears. In general, the main issues are the stability of the flexible rotor under high rotation speed and good disturbance rejection from zero to nominal operating speeds. Simultaneously, AMBs supported rotors are open-loop unstable, multi-input, multi-output (MIMO) systems. Therefore, a feedback control algorithm is required to maintain the stability of these complex mechatronic systems. The general design motivation is to produce rotor-AMB systems that are safe, efficient and reliable. Moreover, the critical vibration modes of the rotordynamic system are a major concern in the design of the magnetic suspension controller. Since the rotor has the maximum vibration amplitudes at these frequencies, great care must be taken to predict and monitor the behavior due to resonance.

II. MODELING

A. Magnetic Circuit Analysis and Magnetic Force

Corresponding to two non-interrelated 3-pole active magnetic bearings of Fig. 1, we can separately analyse single AMB, that means two decoupled bearings actually. By simple circuit analysis, the magnetic flux passing through each pole can be obtained. The derivation and schematic can be referring to [1] for more detailed. Then, by Ampere's law and principle of virtual work, the magnetic force is related to the magnetic flux. In order to discriminate the two magnetic bearing, index "b1" is to indicate magnetic bearing 1, and index "b2" is to indicate magnetic bearing 2. Finally, magnetic force f_z, f_y can be put into a concise form in term of position of rotor z_r, y_r and coil currents i_1, i_2, i_3, and expressed as

$$f_{z_{b1}} = \frac{\gamma}{2}\left(\Phi_{2_{b1}}{}^2 - \Phi_{1_{b1}}{}^2\right) \tag{1}$$

$$f_{z_{b2}} = \frac{\gamma}{2}\left(\Phi_{2_{b2}}{}^2 - \Phi_{1_{b2}}{}^2\right) \tag{2}$$

$$f_{y_{b1}} = \gamma(\Phi_{1_{b1}}\Phi_{2_{b1}}) \tag{3}$$

$$f_{y_{b2}} = \gamma(\Phi_{1_{b2}}\Phi_{2_{b2}}) \tag{4}$$

where

$$\gamma = \frac{4\mu A_m N^2}{3} \tag{5}$$

$$\begin{bmatrix}\Phi_{1_{b1}}\\ \Phi_{2_{b1}}\end{bmatrix} = \frac{-1}{L_{b1}}\begin{bmatrix}2l_0 - z_{r_{b1}} & \sqrt{3}y_{r_{b1}}\\ y_{r_{b1}} & \sqrt{3}\left(2l_0 + z_{r_{b1}}\right)\end{bmatrix}\begin{bmatrix}i_{1_{b1}}\\ i_{2_{b1}}\end{bmatrix} \tag{6}$$

$$\begin{bmatrix}\Phi_{1_{b2}}\\ \Phi_{2_{b2}}\end{bmatrix} = \frac{-1}{L_{b2}}\begin{bmatrix}2l_0 - z_{r_{b2}} & \sqrt{3}y_{r_{b2}}\\ y_{r_{b2}} & \sqrt{3}\left(2l_0 + z_{r_{b2}}\right)\end{bmatrix}\begin{bmatrix}i_{1_{b2}}\\ i_{2_{b2}}\end{bmatrix} \tag{7}$$

$$L_{b1} = 4l_0^2 - (z_{r_{b1}}{}^2 + y_{r_{b1}}{}^2) \tag{8}$$

$$L_{b2} = 4l_0^2 - (z_{r_{b2}}{}^2 + y_{r_{b2}}{}^2) \tag{9}$$

where μ is the magnetic permeability of the air, A_m is the cross section of magnetic pole, N is the number of coil turns, and l_0 is nominal air gap.

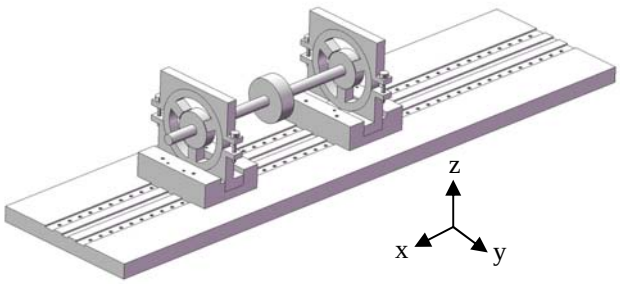

Fig. 1 The schematic of view for 3-pole Rotor-AMBs system

B. Generalized Polynomial Expansion Method

The Generalized Polynomial Expansion Method (G.P.E.M) is a global assumed modes method which describes the deformations of rotating shaft with a series of polynomials. It is assumed that all the deflections and forces are parallel to the $y-z$ plane, and the flexible shaft is approximated by Rayleigh's beam theory. By the assumption, one can express the deflections as function of position along the rotating axis x and time t. Notice that the deflections of rotations and translations are assumed to be small such that the linear elastic theory is valid. Based on G.P.E.M, the translations (V,W) deflections and rotation (B,Γ) along rotating shaft are expressed as a series of polynomial associated with time coefficient functions $a_n(t)$, $b_m(t)$ as

$$V(x,t)=\sum_{n=1}^{N_p} a_n(t)x^{n-1} \tag{10}$$

$$W(x,t)=\sum_{m=1}^{N_p} b_m(t)x^{m-1} \tag{11}$$

$$\mathrm{B}(x,t)=-\sum_{m=2}^{N_p}(m-1)b_m(t)x^{m-2} \tag{12}$$

$$\Gamma(x,t)=\sum_{n=2}^{N_p}(n-1)a_n(t)x^{n-2} \tag{13}$$

where N_p is the number of terms of polynomial. By Lagrangian approach, the governing equations of a general rotor-bearings system can be obtained as

$$\begin{bmatrix}\hat{\mathbf{M}} & 0\\ 0 & \hat{\mathbf{M}}\end{bmatrix}\ddot{\hat{q}}+\Omega\begin{bmatrix}0 & \hat{\mathbf{G}}\\ -\hat{\mathbf{G}} & 0\end{bmatrix}\dot{\hat{q}}+\begin{bmatrix}\hat{\mathbf{K}}_{\mathbf{s}} & 0\\ 0 & \hat{\mathbf{K}}_{\mathbf{s}}\end{bmatrix}\hat{q}=\begin{Bmatrix}\hat{f}_y\\ \hat{f}_z\end{Bmatrix}-\begin{Bmatrix}0\\ \hat{f}_g\end{Bmatrix} \tag{14}$$

where

$$\hat{q}=\{a_1(t)\quad a_2(t)\quad\cdots\quad a_{N_p}(t)\quad b_1(t)\quad b_2(t)\quad\cdots\quad b_{N_p}(t)\}^T \tag{15}$$

$$\hat{\mathbf{M}}(m,n)=\int_0^l\rho\mathrm{A}x^{m+n-2}dx+(m-1)(n-1)\int_0^l I_D x^{m+n-4}dx \tag{16}$$

$$\hat{\mathbf{G}}(m,n)=(m-1)(n-1)\int_0^l I_P x^{m+n-4}dx \tag{17}$$

$$\hat{\mathbf{K}}_{\mathbf{s}}(m,n)=(m-1)(n-1)(m-2)(n-2)\int_0^l EIx^{m+n-6}dx \tag{18}$$

$$\hat{f}_{y_j}=f_{y_{b1}}x_{b1}^{\ j-1}+f_{y_{b2}}x_{b2}^{\ j-1},\ j=1,2,\cdots,N_p \tag{19}$$

$$\hat{f}_{z_j}=f_{z_{b1}}x_{b1}^{\ j-1}+f_{z_{b2}}x_{b2}^{\ j-1},\ j=1,2,\cdots,N_p \tag{20}$$

$$\hat{f}_{g_j}=g\int_0^l\rho(x)A(x)x^{j-1}dx,\ j=1,2,\cdots,N_p \tag{21}$$

where index "j" is represent j-th component of the vector. Note that x_{b1} and x_{b2} are position of magnetic bearing 1 and magnetic bearing 2 along the x axis, and the flexible shaft is of total length l with the distributed parameters of bending stiffness EI, mass per unit length ρA, and cross-section diametral and polar mass moment of inertia per unit length I_D and I_P, and rotating speed Ω, and g is gravitational acceleration. Moreover, the dot denotes differential with respect to time t and the prime denotes differential with respect to axial distance x.

C. Eigen Mode Method

In this section, is to develop an Eigen Mode Method to obtain a mathematical model, the shaft deformation can be expressed as linear combination of the all mode shapes. Using the eigen mode method, $V(x,t)$, $W(x,t)$, $\mathrm{B}(x,t)$ and $\Gamma(x,t)$ can be expressed as

$$V(x,t)=\sum_{i=1}^{N_e} v_i(t)\psi_i(x) \tag{22}$$

$$W(x,t)=\sum_{i=1}^{N_e} w_i(t)\psi_i(x) \tag{23}$$

$$\mathrm{B}(x,t)=-\sum_{i=1}^{N_e} w_i(t)\psi_i'(x) \tag{24}$$

$$\Gamma(x,t)=\sum_{i=1}^{N_e} v_i(t)\psi_i'(x) \tag{25}$$

where N_e is the mode number, $\psi_i(x)$ is mode shape functions that satisfy the corresponding shaft boundary conditions, and $v_i(t)$ and $w_i(t)$ are the respective modal displacements.

Similarly, the governing equations of a general rotor-bearings system can be obtained as

$$\begin{bmatrix}\mathbf{M} & 0\\ 0 & \mathbf{M}\end{bmatrix}\ddot{q}+\Omega\begin{bmatrix}0 & \mathbf{G}\\ -\mathbf{G} & 0\end{bmatrix}\dot{q}+\begin{bmatrix}\mathbf{K}_{\mathbf{s}} & 0\\ 0 & \mathbf{K}_{\mathbf{s}}\end{bmatrix}q=\begin{Bmatrix}f_y\\ f_z\end{Bmatrix}-\begin{Bmatrix}0\\ f_g\end{Bmatrix} \tag{26}$$

where

$$q=\{v_1(t)\quad v_2(t)\quad\cdots\quad v_{N_e}(t)\quad w_1(t)\quad w_2(t)\quad\cdots\quad w_{N_e}(t)\}^T \tag{27}$$

$$\mathbf{M}=\int_0^l\rho A\tilde{\mathbf{M}}\,dx+\int_0^l I_D\tilde{\mathbf{G}}\,dx \tag{28}$$

$$\mathbf{G} = \int_0^l I_P \tilde{\mathbf{G}}\, dx \tag{29}$$

$$\mathbf{K}_s = \int_0^l EI\, \tilde{\mathbf{K}}\, dx \tag{30}$$

$$\tilde{\mathbf{M}}(m,n) = \psi_m(x)\psi_n(x) \tag{31}$$

$$\tilde{\mathbf{G}}(m,n) = \psi'_m(x)\psi'_n(x) \tag{32}$$

$$\tilde{\mathbf{K}}(m,n) = \psi''_m(x)\psi''_n(x) \tag{33}$$

$$f_{y_j} = f_{y_{b1}}\psi_j(x_{b1}) + f_{y_{b2}}\psi_j(x_{b2}) \ , \ j = 1,2,\cdots,N_e \tag{34}$$

$$f_{z_j} = f_{z_{b1}}\psi_j(x_{b1}) + f_{z_{b2}}\psi_j(x_{b2}) \ , \ j = 1,2,\cdots,N_e \tag{35}$$

$$f_{g_j} = g\int_0^l \rho(x)A(x)\psi_j(x)dx \ , \ j = 1,2,\cdots,N_e \tag{36}$$

where index "j" is represent j-th component of the vector.

D. *Comparison of Modeling Method*

At this section, we will discuss and compute the critical speed by G.P.E.M and Eigen Mode Method. To illustrate the efficiency and the accuracy of the Eigen Mode Method, an example of uniform rotor for pinned-pinned boundary condition are studied and the detailed data and results can be refer to [2]. Furthermore, the Campbell diagram for the example in shown in Fig. 2.

At later section, we will try to obtain approximate mode shape functions by numerical techniques (G.P.E.M) as mode shapes of non-uniform rotor system in Eigen Mode Method.

III. *CONTROLLER DESIGN*

A. *State Space Model*

With the arrival of space exploration, requirements for control systems increased in scope. Modeling systems by linear, time-invariant differential equations and subsequent transfer function functions became inadequate. The state-space, approach (also referred to as the modern, or time-domain, approach) is a unified method for modeling, analyzing, and designing a wide range of systems. Many systems do not have just a single input and a single output.

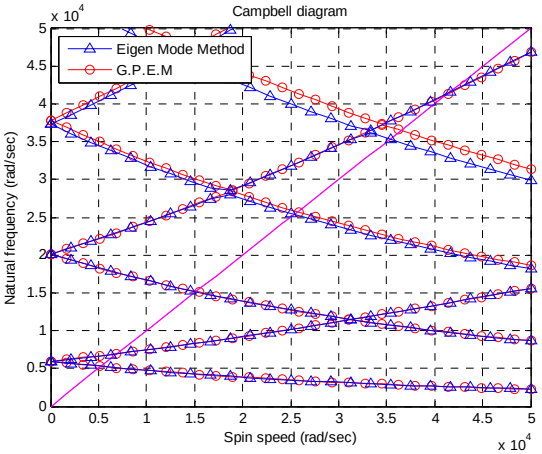

Fig. 2 The Campbell Diagram of $N_e = 4$ and $N_p = 8$ for example

Multiple-input, multiple-output systems can be compactly represented in state space with a model similar in form and complexity to that used for single-input, single-output systems. The state-space approach is also attractive because of the availability of numerous state-space software packages for the personal computer.

From equation of motion (26) and the state space representation for the model of Eigen Mode Method can be expressed as

$$\begin{Bmatrix} \dot{z}_1 \\ \dot{z}_2 \\ \dot{z}_3 \\ \dot{z}_4 \end{Bmatrix} = \begin{Bmatrix} z_2 \\ \mathbf{M}^{-1}\{-\mathbf{K}_s z_1 - \Omega\mathbf{G}z_4\} \\ z_4 \\ \mathbf{M}^{-1}\{-gr_g + \Omega\mathbf{G}z_2 - \mathbf{K}_s z_3\} \end{Bmatrix} + \begin{Bmatrix} 0 \\ \mathbf{M}^{-1}\gamma\left(\Phi_{1_{b1}}\Phi_{2_{b1}}r_{b1} + \Phi_{1_{b2}}\Phi_{2_{b2}}r_{b2}\right) \\ 0 \\ \mathbf{M}^{-1}\dfrac{\gamma}{2}\left[\left(\Phi_{2_{b1}}{}^2 - \Phi_{1_{b1}}{}^2\right)r_{b1} + \left(\Phi_{2_{b2}}{}^2 - \Phi_{1_{b2}}{}^2\right)r_{b2}\right] \end{Bmatrix} \tag{37}$$

where

$$z_1 = v \ , \ z_2 = \dot{v} \ , \ z_3 = w \ , \ z_4 = \dot{w} \tag{38}$$

$$r_{b1} = \begin{Bmatrix} \psi_1(x_{b1}) & \psi_2(x_{b1}) & \cdots & \psi_{N_e}(x_{b1}) \end{Bmatrix}^T \tag{39}$$

$$r_{b2} = \begin{Bmatrix} \psi_1(x_{b2}) & \psi_2(x_{b2}) & \cdots & \psi_{N_e}(x_{b2}) \end{Bmatrix}^T \tag{40}$$

$$r_g = \begin{Bmatrix} \int_0^l \rho(x)A(x)\psi_1(x)dx & \int_0^l \rho(x)A(x)\psi_2(x)dx \\ \cdots & \int_0^l \rho(x)A(x)\psi_{N_e}(x)dx \end{Bmatrix}^T \tag{41}$$

B. *Feedback Linearization*

A feedback linearization approach is taken to design a stabilizing controller for the system given by (37). In other words, it is desired to find a state feedback $i = \phi(x, \tilde{i})$ such that the closed-loop system is linear, i.e.

$$\dot{z} = f\left(z, \phi(z, \tilde{i})\right) = \mathbf{A} + \mathbf{B}\tilde{i} \tag{42}$$

where $\tilde{i}$ is a new input. Fortunately, the special structure of the present system permits a solution to its exact linearization. The idea is to solve for $(\Phi_{1_{b1}}, \Phi_{2_{b1}})$ and $(\Phi_{1_{b2}}, \Phi_{2_{b2}})$, which are regarded as virtual inputs.

From (37), we take the terms which are not related to states and incorporate them into virtual inputs as

$$\tilde{i}_1 = \mathbf{M}^{-1}\gamma\left(\Phi_{1_{b1}}\Phi_{2_{b1}}r_{b1} + \Phi_{1_{b2}}\Phi_{2_{b2}}r_{b2}\right) \tag{43}$$

$$\tilde{i}_2 = \frac{\mathbf{M}^{-1}\gamma}{2}\left[\left(\Phi_{2_{b1}}{}^2 - \Phi_{1_{b1}}{}^2\right)r_{b1} + \left(\Phi_{2_{b2}}{}^2 - \Phi_{1_{b2}}{}^2\right)r_{b2}\right] - g\mathbf{M}^{-1}r_g \tag{44}$$

According to the equation (43)-(44), we know the number of virtual inputs is $2N_e$. In fact, the rotor magnetic bearings system can provide 4 control inputs only, so we define a new input as

$$u_1 = \Phi_{1_{b1}}\Phi_{2_{b1}}\ ,\ u_2 = \Phi_{1_{b2}}\Phi_{2_{b2}} \tag{45}$$

$$u_3 = \Phi_{2_{b1}}{}^2 - \Phi_{1_{b1}}{}^2\ ,\ u_4 = \Phi_{2_{b2}}{}^2 - \Phi_{1_{b2}}{}^2 \tag{46}$$

If equation (45) – (46) is achieved, then substituting them into (37), we can obtain the system which can be linearized to the form as

$$\dot{z} = \mathbf{A}z + \mathbf{B}u - g\begin{bmatrix} 0 \\ 0 \\ 0 \\ \mathbf{M}^{-1} \end{bmatrix} r_g \tag{47}$$

where

$$u = \{u_1 \quad u_2 \quad u_3 \quad u_4\}^T \tag{48}$$

$$\mathbf{A} = \begin{bmatrix} 0 & \mathbf{I} & 0 & 0 \\ -\mathbf{M}^{-1}\mathbf{K}_s & 0 & 0 & -\Omega\mathbf{M}^{-1}\mathbf{G} \\ 0 & 0 & 0 & \mathbf{I} \\ 0 & \Omega\mathbf{M}^{-1}\mathbf{G} & -\mathbf{M}^{-1}\mathbf{K}_s & 0 \end{bmatrix} \tag{49}$$

$$\mathbf{B} = \begin{bmatrix} 0 & 0 & 0 & 0 \\ \gamma\mathbf{M}^{-1}r_{b1} & \gamma\mathbf{M}^{-1}r_{b2} & 0 & 0 \\ 0 & 0 & 0 & 0 \\ 0 & 0 & \dfrac{\gamma\mathbf{M}^{-1}r_{b1}}{2} & \dfrac{\gamma\mathbf{M}^{-1}r_{b2}}{2} \end{bmatrix} \tag{50}$$

Once $(\Phi_{1_{b1}}, \Phi_{2_{b1}})$ and $(\Phi_{1_{b2}}, \Phi_{2_{b2}})$ are solved, the real inputs $(i_{1_{b1}}, i_{2_{b1}})$ and $(i_{1_{b2}}, i_{2_{b2}})$ can be easily obtained by the transformation (6) and (7). There are some possible solutions to (45) and (46) and the below is an admissible solution

$$\Phi_{1_{b1}}(u_1, u_3) = \sqrt{\frac{-u_3 + \sqrt{u_3{}^2 + 4u_1{}^2}}{2}}\,\mathrm{sgn}(u_1) \tag{51}$$

$$\Phi_{2_{b1}}(u_1, u_3) = \sqrt{\frac{u_3 + \sqrt{u_3{}^2 + 4u_1{}^2}}{2}} \tag{52}$$

$$\Phi_{1_{b2}}(u_2, u_4) = \sqrt{\frac{-u_4 + \sqrt{u_4{}^2 + 4u_2{}^2}}{2}}\,\mathrm{sgn}(u_2) \tag{53}$$

$$\Phi_{2_{b2}}(u_2, u_4) = \sqrt{\frac{u_4 + \sqrt{u_4{}^2 + 4u_2{}^2}}{2}} \tag{54}$$

$$\mathrm{sgn}(a) = \begin{cases} 1 & a \geq 0 \\ -1 & a < 0 \end{cases} \tag{55}$$

Note that the sign function given here is different from the usual one since $\mathrm{sgn}(0) = 1$ to avoid singularity. Finally, the true input currents $(i_{1_{b1}}, i_{2_{b1}})$ and $(i_{1_{b2}}, i_{2_{b2}})$ now read

$$\begin{bmatrix} i_{1_{b1}} \\ i_{2_{b1}} \end{bmatrix} = \frac{-1}{\sqrt{3}}\begin{bmatrix} \sqrt{3}(2l_0 + W(x_{b1}, t)) & -\sqrt{3}V(x_{b1}, t) \\ -V(x_{b1}, t) & 2l_0 - W(x_{b1}, t) \end{bmatrix}\begin{bmatrix} \Phi_{1_{b1}} \\ \Phi_{2_{b1}} \end{bmatrix} \tag{56}$$

$$\begin{bmatrix} i_{1_{b2}} \\ i_{2_{b2}} \end{bmatrix} = \frac{-1}{\sqrt{3}}\begin{bmatrix} \sqrt{3}(2l_0 + W(x_{b2}, t)) & -\sqrt{3}V(x_{b2}, t) \\ -V(x_{b2}, t) & 2l_0 - W(x_{b2}, t) \end{bmatrix}\begin{bmatrix} \Phi_{1_{b2}} \\ \Phi_{2_{b2}} \end{bmatrix} \tag{57}$$

where

$$V(x_{b1}, t) = z_1{}^T r_{b1}\ ,\ W(x_{b1}, t) = z_3{}^T r_{b1} \tag{58}$$

$$V(x_{b2}, t) = z_1{}^T r_{b2}\ ,\ W(x_{b2}, t) = z_3{}^T r_{b2} \tag{59}$$

At fact, we can determine the analytical bias virtual control current, and it mainly cancels out the effects which caused by gravitation, due to nominal system (37). First of all, the idea is to compute the virtual control input when states of steady state located on the desired equilibrium point analytically, it will be neglected here. As a result of 4 virtual control inputs u_1, u_2, u_3, u_4, we can see that the equilibrium points are not exactly zero when N_e more than 2.

C. Robust Control (I.S.M.C)

The feedback linearization is based on perfect models, which are almost impossible to exist in practice. A more reasonable assumption is that real system model is nominal one plus a bounded uncertain part $\Delta f(z, \phi(z,u))$. In what follows, quantities of the nominal system are represented with an "$\frown$". The feedback linearization control currents (56) and (57) should also use the nominal parameters. Upon applying (56) – (57), equation (37) becomes

$$\dot{z} = \widehat{f}(z, \phi(z,u)) + \Delta f(z, \phi(z,u)) \tag{60}$$

Lyapunov-based control methods such as Lyapunov redesign, sliding mode control, adaptive control, etc, can be used to achieve robust stabilization. In this paper, an integral sliding mode controller will be designed to allow for large uncertainties and to achieve good steady-state accuracy. To facilitate the controller design, equation (60) is rewritten in the regular form as

$$\dot{\eta} = \xi \tag{61}$$

$$\dot{\xi} = \widehat{f}_a(\eta, \xi) + \mathbf{G}_a\left[u + \delta_{\xi}(\eta, \xi, u)\right] \tag{62}$$

where

$$\eta = [\eta_1^T \quad \eta_2^T] = [z_1^T \quad z_3^T] \tag{63}$$

$$\xi = [\xi_1^T \quad \xi_2^T] = [z_2^T \quad z_4^T] \tag{64}$$

$$\mathbf{G}_a = \begin{bmatrix} \gamma\mathbf{M}^{-1}r_{b1} & \gamma\mathbf{M}^{-1}r_{b2} & 0 & 0 \\ 0 & 0 & \dfrac{\gamma\mathbf{M}^{-1}r_{b1}}{2} & \dfrac{\gamma\mathbf{M}^{-1}r_{b2}}{2} \end{bmatrix} \tag{65}$$

where $\eta \in IR^{n-p}$, $\xi \in IR^p$, $u \in IR^p$, and $\delta_{\xi}(\eta, \xi, u)$ is unknown smooth functions of η, ξ and u, representing uncertainties or disturbances. It is obvious that the uncertainty $\delta_{\xi}(\eta, \xi, u)$ satisfies the matching condition. Assume that $\mathbf{G}_a$ is nonsingular in the domain of interest and invertible. So the subsequent derivation is based on $N_e \leq 2$ in this paper. The integral sliding mode control takes an integral sliding manifold

$$\sigma = \xi + b_1\eta + b_2 z_m\ ,\ \dot{z}_m = \eta \tag{66}$$

where b_1 and b_2 are positive constants. The strategy of integral sliding mode control is only required to maintain $\dot{\sigma} = 0$ (or $\sigma =$ constant). Therefore, η and hence ξ will approach zero asymptotically. To this aim, the control input u consists of equivalent control u_{eq} and switching control u_s.

$$u = u_{eq} + u_s \tag{67}$$

The equivalent control u_{eq} is to maintain the condition $\dot{\sigma} = 0$, in the absence of uncertainty, and obtained as

$$u_{eq} = \mathbf{G}_a^{-1}\left(-\tilde{\mathbf{A}}\begin{Bmatrix}\eta_1\\ \xi_1\\ \eta_2\\ \xi_2\end{Bmatrix} - b_1\begin{Bmatrix}\xi_1\\ \xi_2\end{Bmatrix} - b_2\begin{Bmatrix}\eta_1\\ \eta_2\end{Bmatrix}\right) \tag{68}$$

where

$$\tilde{\mathbf{A}} = \begin{bmatrix} -\mathbf{M}^{-1}\mathbf{K} & 0 & 0 & -\Omega\mathbf{M}^{-1}\mathbf{G} \\ 0 & \Omega\mathbf{M}^{-1}\mathbf{G} & -\mathbf{M}^{-1}\mathbf{K} & 0 \end{bmatrix} \tag{69}$$

When the system states are not on the sliding manifold initially, the switching control u_s is applied to force them reaching $\dot{\sigma} = 0$ in finite time. Bringing back the uncertainties and $\dot{\sigma}$ become

$$\dot{\sigma} = \mathbf{G}_a u_s + \mathbf{G}_a \delta_\xi(\eta, \xi, u_s + u_{eq}) \tag{70}$$

where $\mathbf{G}_a \delta_\xi(\eta, \xi, u_s + u_{eq}) = \Delta(\eta, \xi, u)$. Suppose that within the AMB's operational domain, an upper bound on the uncertainty $\Delta(\eta, \xi, u)$ is known

$$\left\|\Delta(\eta, \xi, u)\right\|_\infty \le \rho_c + k_c \left\|u\right\|_\infty \tag{71}$$

where $\rho_c \ge 0$ amounts to the estimate on the open loop uncertainty. It is not restricted to be small here. On the other hand, $0 \le k_c < 1$ represents the bound on control-related uncertainty. It cannot exceed the magnitude of the real control to prevent from losing control authority. With the uncertainty bounds given by (71) and utilizing Lyapunov function candidates $V_j = \frac{1}{2}\sigma_j^2$ for $j = 1 \sim 4$, we can obtain

$$\dot{V}_j = \sigma_j \dot{\sigma}_j \le \sigma_j [\mathbf{G}_a u_s + \mathbf{G}_a \delta_\xi(\eta, \xi, u_s + u_{eq})] \tag{72}$$

by the estimation (73), the switching control can be designed as

$$u_s = -\mathbf{G}_a^{-1}\left(\frac{\rho_c + \alpha}{1 - k_c}\right)\left[sat(\frac{\sigma_1}{\varepsilon}) \quad sat(\frac{\sigma_2}{\varepsilon}) \quad sat(\frac{\sigma_3}{\varepsilon}) \quad sat(\frac{\sigma_4}{\varepsilon})\right]^{\mathrm{T}} \tag{73}$$

where α and ε are positive constants, and $sat(\sigma_j/\varepsilon)$ is the saturation function. Finally, yielding a overall closed-loop system with bias virtual control input

$$\begin{Bmatrix}\dot{z}_1\\ \dot{z}_2\\ \dot{z}_3\\ \dot{z}_4\end{Bmatrix} = \mathbf{A}\begin{Bmatrix}z_1\\ z_2\\ z_3\\ z_4\end{Bmatrix} - \mathbf{B}\mathbf{G}_a^{-1}\tilde{\mathbf{A}}\begin{Bmatrix}z_1\\ z_2\\ z_3\\ z_4\end{Bmatrix} - b_1\mathbf{B}\mathbf{G}_a^{-1}\begin{Bmatrix}z_2\\ z_4\end{Bmatrix} - b_2\mathbf{B}\mathbf{G}_a^{-1}\begin{Bmatrix}z_1\\ z_3\end{Bmatrix}$$

$$-\mathbf{B}\mathbf{G}_a^{-1}\left(\frac{\rho + \alpha}{1 - k}\right)\begin{Bmatrix} sat\left(\frac{\sigma_1}{\varepsilon}\right)\\ sat\left(\frac{\sigma_2}{\varepsilon}\right)\\ sat\left(\frac{\sigma_3}{\varepsilon}\right)\\ sat\left(\frac{\sigma_4}{\varepsilon}\right)\end{Bmatrix} + \mathbf{B}\tilde{u} \tag{74}$$

$$\dot{z}_m = \begin{Bmatrix} z_1 \\ z_3 \end{Bmatrix} \tag{75}$$

IV. SIMULATION

A. Descriptions of Magnetic Flexible Rotor Bearing System

The magnetic flexible rotor bearing system is supported by two 3-pole active magnetic bearings, and the schematic view is shown in Fig. 3, and one end connect to motor. For all simulations in this section, the system parameters and geometric sizes are given in Table I and Table II. It is obvious that the rotor is belonging to non-uniform shaft, mainly including different cross section and density of material along x axis.

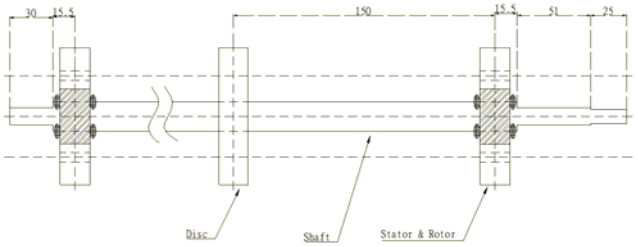

Fig. 3 The schematic view of magnetic flexible rotor bearing system

Table I
Parameters of system and magnetic bearing

Nominal air gap, l_0	3×10^{-4} m
Magnetic permeability of the air, μ	$4\pi\times10^{-7}$ N/A^2
Gravitational acceleration, g	9.81 m/s^2
Cross section of magnetic pole, A_m	2.1×10^{-4} m^2
Number of coil turns, N	150
Operating speed, Ω	10000 rpm

B. Computation of Mode Shapes by G.P.E.M

In order to obtain a set of mode shapes for non-uniform rotor, Generalized Polynomial Expansion Method (G.P.E.M) is applied to compute numerical solutions here.

Table II
Geometric sizes and configuration data of the rotating shaft

Shaft	Axial Location (mm)	Radius (mm)	Density (Kg/m^3)	Elastic Modulus (N/m^2)
1	0 ~ 40.0	15.5	2800	6.9×10^{10}
2	40.0 ~ 45.5	4.0	7800	2.1×10^{11}
3	45.5 ~ 96.5	5.85	7800	2.1×10^{11}
4	96.5 ~ 101.5	10.0	7800	2.1×10^{11}
5	101.5 ~ 122.5	18.7	7800	2.1×10^{11}
6	122.5 ~ 252.0	10.0	7800	2.1×10^{11}
7	252.0 ~ 272.0	47.0	2087	7.86×10^{10}
8	272.0 ~ 404.5	10.0	7800	2.1×10^{11}
9	404.5 ~ 425.5	18.7	7800	2.1×10^{11}
10	425.5 ~ 430.5	10.0	7800	2.1×10^{11}
11	430.5 ~ 460.5	5.85	7800	2.1×10^{11}

Remarks:

- Shaft 1 is Coupling, shaft 5 and 9 is Magnetic Bearing , Shaft 7 is Disk
- Density and Elastic Modulus of shaft 7 is equivalent data due to volume ratio of aluminum and stainless steel

Although the mode shape which obtained by using G.P.E.M is not exact eigen mode of flexible rotor, the orthogonality of first two mode shapes still located in acceptable range due to issue of model reduction. In addition, we take $N_p = 8$ and the corresponding coefficients of polynomial and orthogonality for mode shapes are shown in the Table III and Table IV, and the representation of mode shape with fixed-free boundary condition can be expressed as

$$\psi_i(x) = a_3x^2 + a_4x^3 + a_5x^4 + a_6x^5 + a_7x^6 + a_8x^7 \qquad (76)$$

Note that the subscripts ' i ' is represent i -th mode. Furthermore, the first two mode shapes will be shown in Fig. 4.

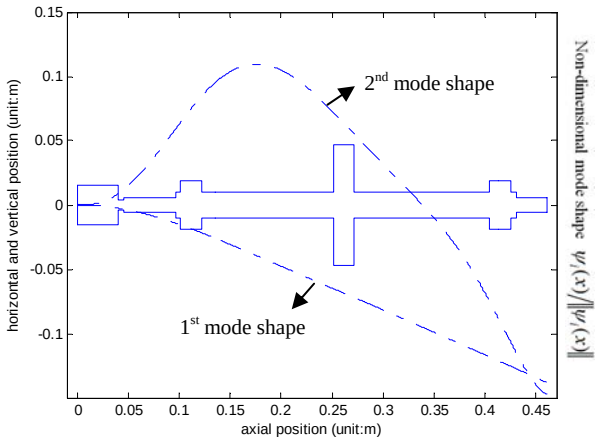

Fig. 4 The first two mode shape by G.P.E.M with $N_p = 8$

Next, take the equation (76) as a set of mode shapes of Eigen Mode Method, then can determine the Eigenvalue problem and solve the corresponding Eigenvalue and Eigenvector, and the results of $N_e = 3$ are listed in Table III, let us to know and understand about the orthogonality of mode shapes.

Table III
The coefficients of polynomial for mode shapes $N_p = 8$

i -th	a_3	a_4	a_5	a_6	a_7	a_8
1	-0.00209	-0.01297	0.13843	-0.47769	0.74501	-0.44434
2	0.00001	0.01105	-0.11210	0.43204	-0.74912	0.48936
3	0.00151	-0.00499	0.00097	-0.14446	0.66677	-0.73111
4	-0.00149	0.02546	-0.16326	0.49934	-0.73724	0.42406
5	-0.00080	0.01670	-0.12676	0.44782	-0.74675	0.47484
6	0.00056	-0.01255	0.10374	-0.40284	0.74274	-0.52453

Table IV
The Eigenvalue λ_i and Eigenvector of $N_e = 3$ for $\lambda = 1$

$\sqrt{\lambda_i}$	0.0515358×10^4	0.4254686×10^4	1.0956283×10^4
Eigenvector	$\begin{Bmatrix} 1.000000000 \\ 0.000000513 \\ -0.000000049 \end{Bmatrix}$	$\begin{Bmatrix} -0.000023766 \\ -1.000000000 \\ -0.000001645 \end{Bmatrix}$	$\begin{Bmatrix} -0.000000911 \\ -0.000000667 \\ 1.000000000 \end{Bmatrix}$

C. *Uncertainties for Unmodeled Higher Order Dynamics*

In this case, we will simulate a higher order system of $N_e = 3$ as real plant, our aim and strategy is to implement Integral Sliding Mode controller which is designed by $N_e = 2$ to overcome such uncertainties, and examine the performance of controller and Eigen Mode Method. Note that bias virtual control current $\tilde{u}$ which caused by gravitation still is computed by $N_e = 2$.

Moreover, the parameters of I.S.M.C controller are listed on Table V, mainly provided by trial and error. The results of numerical simulation are shown in Fig. 5~10, including trajectory of rotor on the magnetic bearings, and the control current $i_{1_{b1}}$, $i_{2_{b1}}$, $i_{1_{b2}}$, $i_{2_{b2}}$.

Table V
The parameters of the I.S.M.C controller for Case 1

b_1	b_2	ρ_c	α	k_c	ε
50	150	150	20	0.7	0.2

IV. CONCLUSIONS

In simulation, we must be able to embed the uncertainties into the nominal system and stabilize the system within our considerations and specifications, as well as verify the feasibility of modeling method and I.S.M.C. According to the results of simulations, we can know that the influence of various uncertainties, such as contribution of higher order dynamic.

From the results, we also can see slightly that the displacements of rotor which located on magnetic bearings

on steady state are not equal to zero exactly, mainly caused by the contribution of third elastic mode. Regarding to method of simulate close loop system due to this such uncertainties, we assume that enable to observe all states, and drop the states of third elastic mode, then feedback the states of first and second elastic mode only.

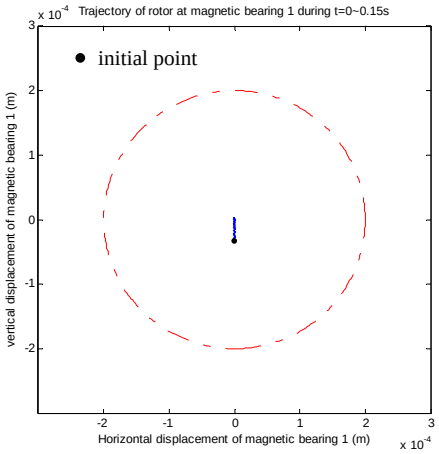

Fig. 5 Trajectory of rotor at magnetic bearing 1

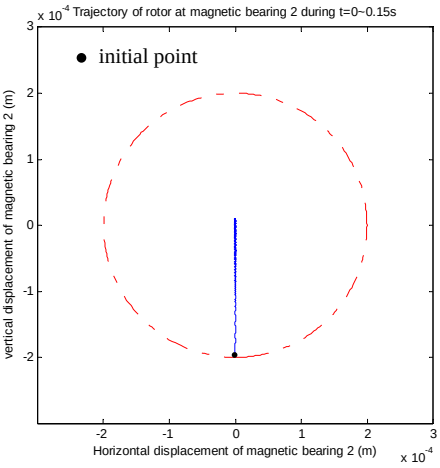

Fig. 6 Trajectory of rotor at magnetic bearing 2

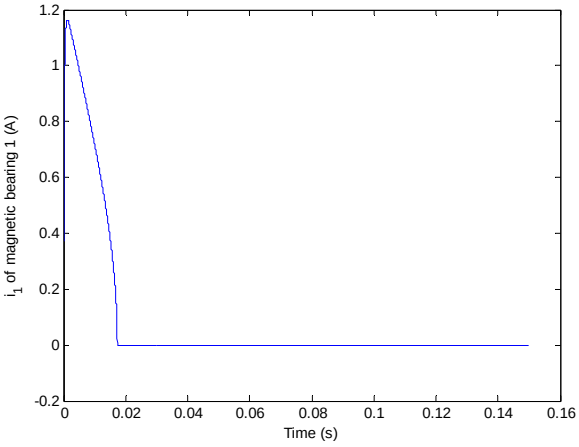

Fig. 7 Control Current $i_{1_{b1}}$ during $t = 0 \sim 0.15s$

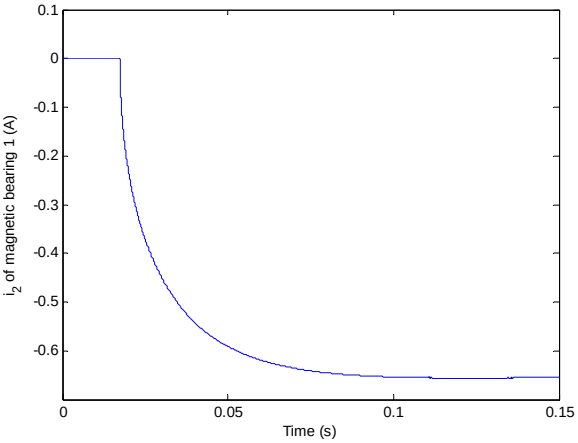

Fig. 8 Control Current $i_{2_{b1}}$ during $t = 0 \sim 0.15s$

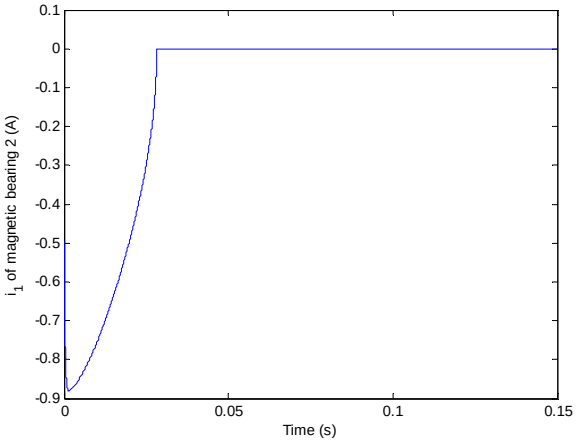

Fig. 9 Control Current $i_{1_{b2}}$ during $t = 0 \sim 0.15s$

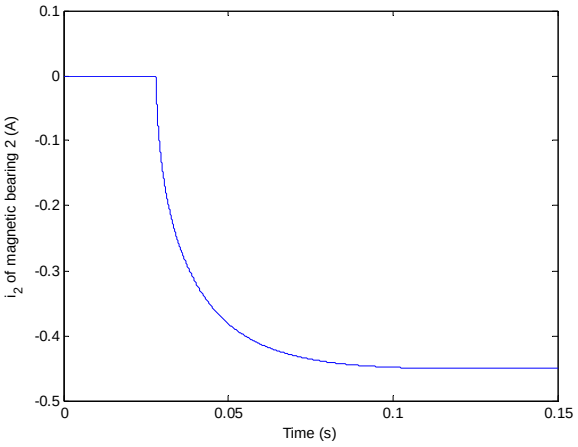

Fig. 10 Control Current $i_{2_{b2}}$ during $t = 0 \sim 0.15s$

REFERENCES

[1] C.T. Hsu and S.L. Chen, "Optimal Design, Modeling and Control of a 3-Pole Active Magnetic Bearing System," *PhD Th esis o f National Chung Cheng University*, 2002, pp. 1-50

[2] J. L. Hwang, "Vibration Analysis of Rotordynamic Systems with Generalized Polynomial Expansion Method," *PhD Th esis o f*

National Cheng Kung University , December 1990, pp. 10-74 and pp. 175-186

[3] L.W. Chen and D.M. Ku, “Finite Element Analysis of Natural Whirl Speeds of Rotating Shafts,” *Computers & Structures* , Vol.40, No. 3, 1991, pp. 741-747

[4] C.C. Cheng and J.K. Lin, “Modelling a rotating shaft subjected to a high-speed moving force,” *Journal of sound and vibration* , 2003, Vol.261, pp.955-965

[5] U.C. Gu and C.C. Cheng, “Vibration analysis of a high-speed spindle under the action of a moving mass,” *Journal of Sound and Vibration*, 2004, Vol.278, pp. 1131-1146

[6] I. Arredondo, J. Jugo and V. Etxebarria, “Modeling and control of a flexible rotor system with AMB-based sustentation,” *ISA Transactions*, Vol.47, 2008, pp. 101-112

[7] N. Tanaka, T. Watanabe and K. Seto, “Levitation and Vibration Control of a Flexible Rotor by using Active Magnetic Bearing,” *11th I nternational Symposium on Magnetic Bearings*, August, Japan, pp. 26-29

[8] M.J. Jang, C.L. Chen and Y.M. Tsao, “Sliding mode control for active magnetic bearing system with flexible rotor,” *Journal of the Franklin Institute*, Vol. 342, 2005, pp. 401-419